**SUPPORTING INFORMATION**

# Gating residues govern ligand unbinding kinetics from the buried cavity in HIF2$\alpha$ PAS-B

Marion L. Silvestrini[1,‡], Riccardo Solazzo[2,‡], Soumendu Boral[3], Melanie J. Cocco[4,5], Joseph D. Closson[3,6], Matteo Masetti[2], Kevin H. Gardner[3,7,8], Lillian T. Chong[1]*

[1]Department of Chemistry, University of Pittsburgh, Pittsburgh, PA
[2]Department of Pharmacy and Biotechnology, Alma Mater Studiorum-Universita di Bologna, Bologna, Italy
[3]Structural Biology Initiative, CUNY Advanced Science Research Center, New York, NY
[4]Department of Pharmaceutical Sciences, University of California, Irvine, Irvine, CA
[5]Department of Molecular Biology and Biochemistry, University of California, Irvine, Irvine, CA
[6]Ph.D. Program in Biochemistry, CUNY Graduate Center, New York, NY
[7]Department of Chemistry and Biochemistry, City College of New York, New York, NY
[8]Ph.D. Programs in Biochemistry, Biology, and Chemistry, CUNY Graduate Center, New York, NY

‡ equal authorship
* corresponding author: ltchong@pitt.edu

## SUPPLEMENTARY COMPUTATIONAL METHODS

**Table S1. GAFF2 force field parameters for the THS-017 small-molecule ligand.**

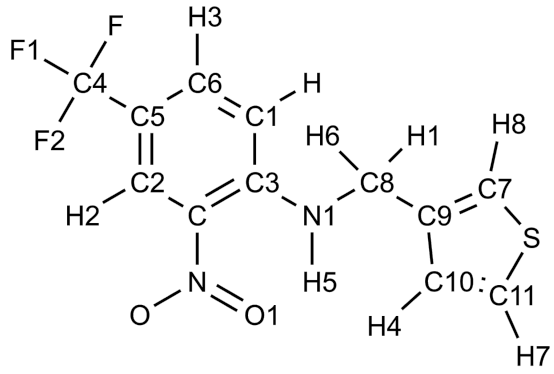


| Atom Name | Atom Type | Partial Atomic Charges |
|---|---|---|
| O1 | O | -0.455436 |
| N | NO | 0.727744 |
| O | O | -0.455436 |
| C | CA | -0.044264 |
| C2 | CA | -0.139585 |
| C5 | CA | -0.097951 |
| C4 | C3 | 0.647155 |
| F/F1/F2 | F | -0.216192 |
| C6 | CA | -0.217631 |
| C1 | CA | -0.021155 |
| H | HA | 0.110423 |
| H3 | HA | 0.191878 |
| H2 | HA | 0.208052 |
| C3 | CA | 0.070686 |

| | | |
|---|---|---|
| N1 | NU | -0.290342 |
| H5 | HN | 0.308434 |
| C8 | C3 | -0.181444 |
| H1/H6 | H1 | 0.112657 |
| C9 | CC | 0.225884 |
| C7 | CD | -0.397909 |
| H8 | H4 | 0.263878 |
| S | SS | 0.037376 |
| C11 | CD | -0.275968 |
| H7 | H4 | 0.247278 |
| C10 | CC | -0.196193 |
| H4 | HA | 0.157787 |

**Table S2. Affinities of HIF-2α PAS-B variants for the THS-017 and THS-020 small-molecule ligands.** Reported values are averages of three independent experiments, using the standard deviations of these measurements to represent the error.

| HIF-2α PAS-B variant | THS-017 | THS-020 |
|---|---|---|
| Wildtype (N288) | $K_d$: 0.60 ± 0.06 μM | $K_d$: 1.35 ± 0.11 μM |
| N288A | $K_d$: 0.50 ± 0.04 μM | $K_d$: 0.84 ± 0.05 μM |
| N288Q | $K_d$: 0.75 ± 0.08 μM | $K_d$: 1.57 ± 0.07 μM |

**Table S3. Thermodynamic parameters for HIF-2α PAS-B ligand-binding.** Reported values are averages of three independent experiments with uncertainties represented by one standard deviation.

| HIF-2α PAS-B variant | THS-017 (kcal/mol) | THS-020 (kcal/mol) |
|---|---|---|
| Wildtype (N288) | ΔG: -8.43 ± 0.5<br>ΔH: -7.03 ± 0.12<br>TΔS: 1.44 ± 0.15 | ΔG: -8.04 ± 0.21<br>ΔH: -8.31 ± 0.16<br>TΔS: -0.30 ± 0.04 |
| N288A | ΔG: -8.54 ± 0.45<br>ΔH: -7.31 ± 0.11<br>TΔS: 1.25 ± 0.08 | ΔG: -8.29 ± 0.17<br>ΔH: -7.24 ± 0.14<br>TΔS: 1.04 ± 0.07 |
| N288Q | ΔG: -8.25 ± 0.35<br>ΔH: -5.65 ± 0.21<br>TΔS: 2.58 ± 0.12 | ΔG: -8.05 ± 0.11<br>ΔH: -8.75 ± 0.18<br>TΔS: -0.68 ± 0.03 |

**Table S4. Kinetics of small-molecule ligand binding and release to HIF-2α PAS-B variants.** Note that the values determined here for ligand binding to wildtype HIF-2α PAS-B are quite similar to values previously reported by Key *et al.* (Key et al. 2009). Reported values are averages of independent fits to eight different residues in the ZZ-exchange spectra, using the standard deviations of these measurements to represent the error.

| Protein | THS-017 | THS-020 |
|---|---|---|
| Wildtype PAS-B | $k_{on}$: (1.45 ± 0.13) x $10^6$ $M^{-1}$ $s^{-1}$<br>$k_{off}$: 1.06 ± 0.08 $s^{-1}$ | $k_{on}$: (1.60 ± 0.26) x $10^6$ $M^{-1}$ $s^{-1}$<br>$k_{off}$: 2.82 ± 0.16 $s^{-1}$ |
| N288A-PAS-B | $k_{on}$: (1.60 ± 0.13) x $10^6$ $M^{-1}$ $s^{-1}$<br>$k_{off}$: 1.45 ± 0.05 $s^{-1}$ | $k_{on}$: (1.76 ± 0.05) x $10^6$ $M^{-1}$ $s^{-1}$<br>$k_{off}$: 3.37 ± 0.17 $s^{-1}$ |
| N288Q-PAS-B | $k_{on}$: (1.34 ± 0.13) x $10^6$ $M^{-1}$ $s^{-1}$<br>$k_{off}$: 0.79 ± 0.06 $s^{-1}$ | $k_{on}$: (1.42 ± 0.08) x $10^6$ $M^{-1}$ $s^{-1}$<br>$k_{off}$: 2.36 ± 0.17 $s^{-1}$ |
| [#]Wildtype PAS-B | [#]$k_{on}$: (1.39 ± 0.22) x $10^6$ $M^{-1}$ $s^{-1}$<br>[#]$k_{off}$: 1.4 ± 0.3 $s^{-1}$ | [#]$k_{on}$: (1.30 ± 0.1) x $10^6$ $M^{-1}$ $s^{-1}$<br>[#]$k_{off}$: 2.5 ± 0.1 $s^{-1}$ |

[#]Values from Key *et al.* (Key et al. 2009)

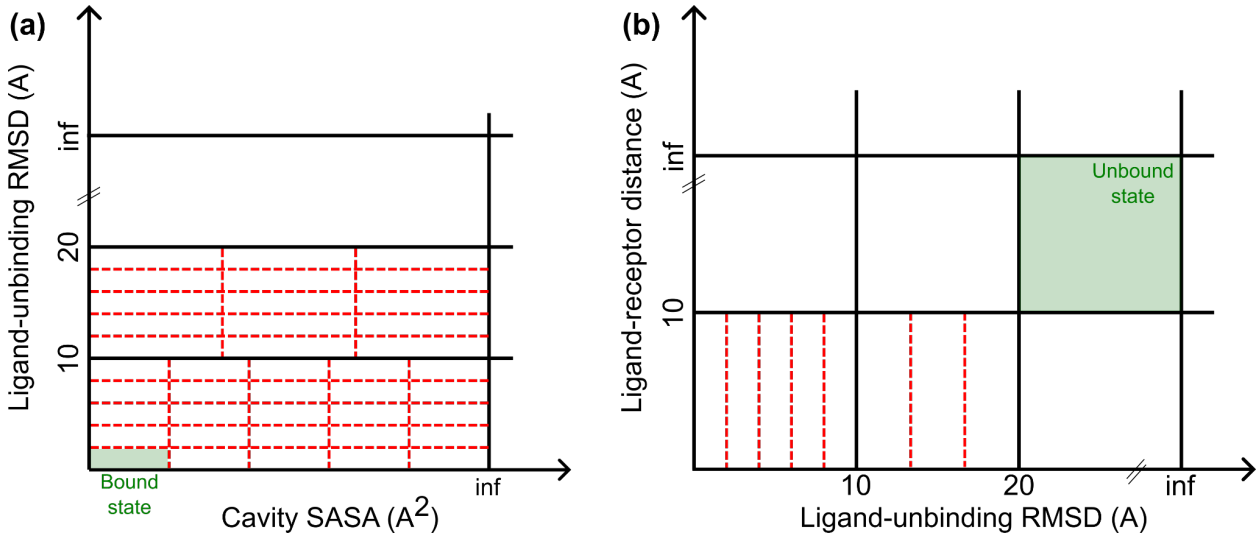


**Figure S1. Schematic diagrams of the two-stage minimal adaptive binning (MAB) scheme used for WE simulations of the THS-017 ligand-unbinding process.** As mentioned in Methods, the WE simulations employed a three-dimensional progress coordinate consisting of (i) the cavity solvent accessible surface area (SASA) of the receptor, (ii) ligand-unbinding RMSD, and (iii) ligand-receptor distance. The first stage of the MAB scheme involved trajectories with a ligand-unbinding RMSD < 10A and the second stage involved trajectories with a ligand-unbinding RMSD > 10A. In both stages, a single bin was used for the ligand-receptor distance. Multiple bins were adaptively positioned along the two other dimensions of the coordinate as follows. **(a)** In the first stage, we used five adaptively positioned bins for both the cavity SASA and ligand-unbinding RMSD. **(b)** In the second stage, we used 3 adaptively positioned bins for the cavity SASA and 5 adaptively positioned bins for the ligand-unbinding RMSD.

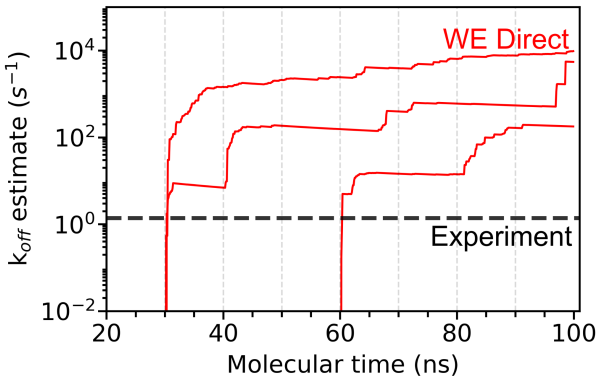


**Figure S2. Assessing $k_{off}$ convergence.** Time-evolution of the estimated $k_{off}$ for THS-017 ligand-unbinding from the three WE simulations (red) as a function of molecular time $N\tau$ where $N$ is the number of WE iterations and $\tau$ is the resampling time interval. Vertical gray lines indicate application of the WESS reweighting procedure (see Methods). The dashed horizontal black line is the experimental $k_{off}$ value.

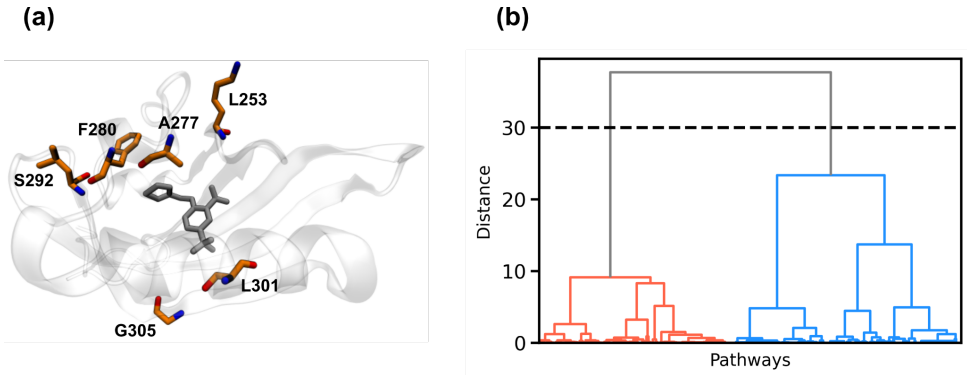


**Figure S3. Clustering of THS-017 ligand-unbinding pathways. (a)** Potential ligand exit points defined by six residues beyond the receptor cavity that are positioned on different secondary structure elements (K253, A277, F280, S292, G305 and L310). **(b)** Dendrogram resulting from hierarchical agglomerative clustering of ligand unbinding pathways using a distance metric based on the Gestalt pattern matching algorithm (see Methods). Two pathway classes, classes 1 (blue) and 2 (red), were identified by positioning a horizontal line (black) at y=30 that divides the dendrogram vertically between nodes with a maximum distance separation.

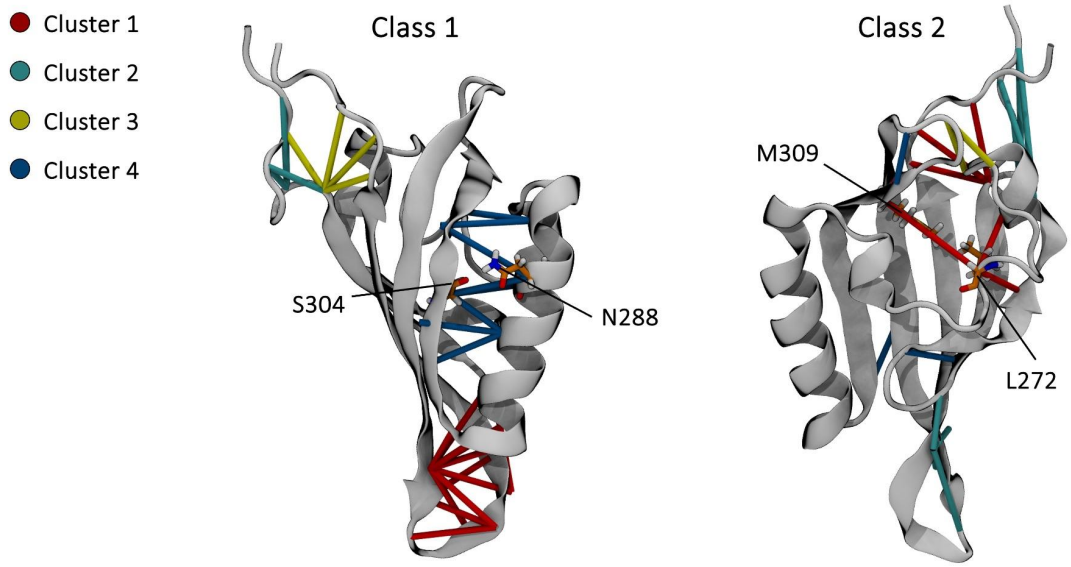


**Figure S4. Inter-residue contacts that are correlated with THS-017 ligand-unbinding.** The most populated clusters of inter-residue contacts (lines) within the HIF2$\alpha$ PAS domain that were identified to be correlated with drug binding using the Leiden network clustering method (see Methods). Based on these clusters, we identified two pairs of conformational gating residues: N288 and S304 in pathway class 1, and L272 and M309 in pathway class 2.

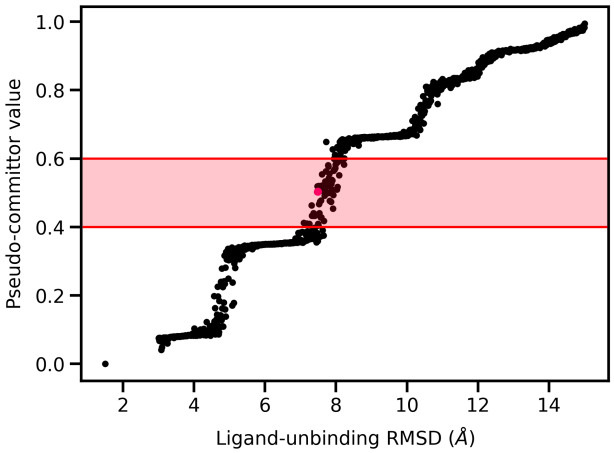


**Figure S5. Pseudo-committor analysis for defining the transition-state ensemble for forming an encounter-complex intermediate in the THS-017 ligand-unbinding process.** The transition-state ensemble (TSE) was defined as having pseudo-committor values of 0.4-0.6 (shaded pink region; see Methods).

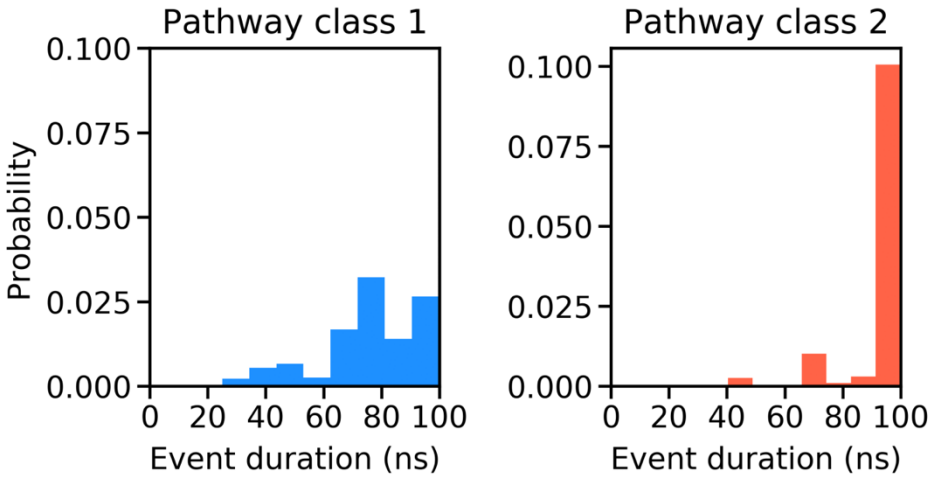


**Figure S6. Probability distribution of event duration times for pathway classes 1 and 2 of the THS-017 ligand unbinding process.** The most probable event durations (barrier-crossing times) of pathways in pathway class 1 are shorter (more direct) than those of pathway class 2.

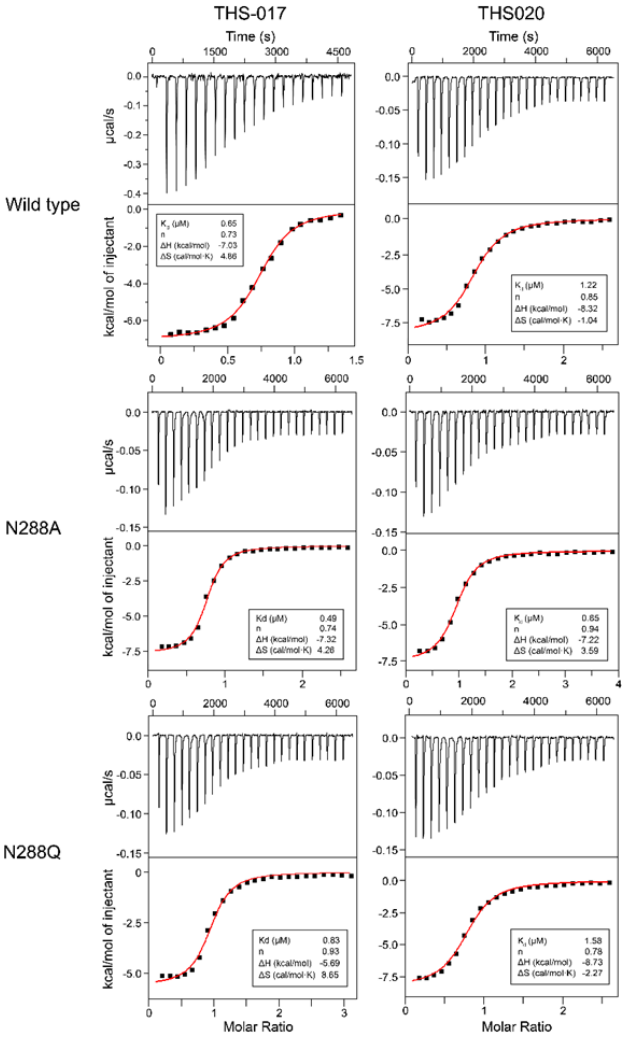


**Figure S7. ITC data showing the thermodynamic parameters of complex formation between HIF-2α PAS-B variants and small-molecule ligands (THS-017 and THS-020).** Data shown is from one of the three runs that were performed for calculation of affinities of HIF-2α PAS-B variants with the THS-017 and THS-020 small-molecule ligands.

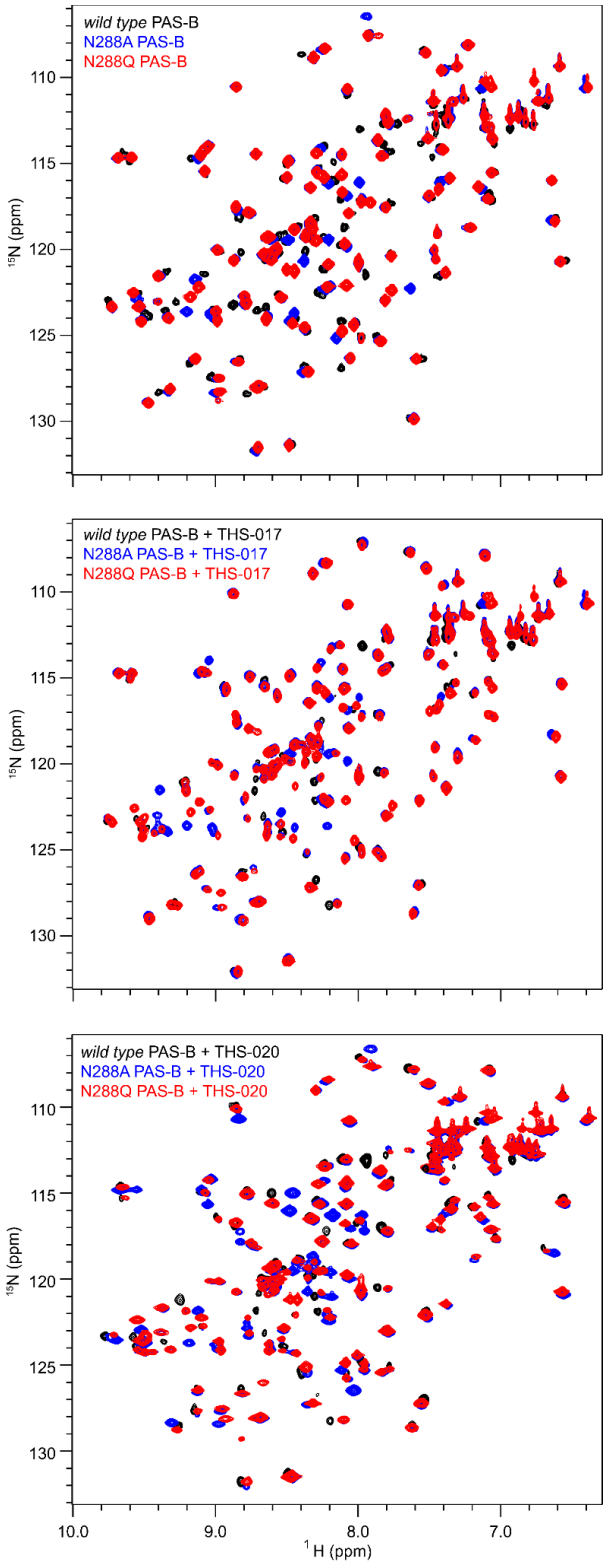


**Figure S8.** 15N-1H HSQC NMR spectra of the apo and ligand-bound forms of wildtype and mutant HIF-2α PAS-B. Minimal changes in the spectra among the wildtype, N288A, and N288Q mutants indicate that the overall fold of HIF-2α PAS-B remains unaltered by the N288 mutations.

**Movies S1-S2.** Movies of the most probable ligand-unbinding pathways for **(S1)** pathway class 1 with conformational gating residues, N288 in the F$\alpha$ helix (magenta) and S304 in the G$\beta$ strand (cyan), and **(S2)** pathway class 2 with conformational gating residues, L272 in the D$\alpha$ helix (magenta) and M309 in the G$\beta$ strand (cyan). The THS-017 ligand and gating residues are highlighted using van der Waals representations.

## SUPPLEMENTARY REFERENCES

Key J, Scheuermann TH, Anderson PC, Daggett V, Gardner KH. 2009. Principles of ligand binding within a completely buried cavity in HIF2alpha PAS-B. J Am Chem Soc. 131(48):17647-17654.